High-Resolution Micro Force Sensing Using a Microbubble Probe Resonator

Bonan Liu, Qiang Zhang, Shen Liu, Changrui Liao, *Member, IEEE*, Junlan Zhong, Jun He, and Yiping Wang, *Senior Member, IEEE*

***Abstract*—High-resolution measurement of forces in micro/nano scale is essential to various applications. A novel miniature force sensor based on a whispering-gallery-mode (WGM) microbubble probe resonator (MPR) is presented in this work. The resonator consists of a thin-wall microbubble and a probe. The highest quality factor obtained is 1.10×10^7. Predominately, the MPR achieves a promising force sensitivity of 19.7 pm/mN and a dynamic range of 0-36 mN. The MPR was used to measure the Young's modulus of a single mode optical fiber (SMF), and the result is coincided with the reported value. High force resolution and spatial resolution are achieved simultaneously. The sensor shows considerable performance and exhibits a potential in micro-force sensing and related applications such as material examination and Young's modulus measurement.**

***Index Terms*—Force sensor, optical fiber sensor, whispering gallery mode resonator.**

I. Introduction

FORCE sensing is a crucial demand in applications such as micro-systems [1], medicine [2], micro-fluidic systems [3]. Over the past decade, a variety of micro-electro-mechanical system (MEMS) force sensors have been proposed, including capacitive-force sensors [4], piezoelectric-type sensors [5], and piezoresistive-force sensors [6]. However, MEMS force sensors are limited in practice for their poor electromagnetic interference resistance, incompatibility towards conductive liquid environment and the geometry of rectangular chips which require proper packaging and electrical connections. Comparatively speaking, optical fiber sensors are predominant for the advantages of compact size, electromagnetic interference immunity, high sensitivity and compatibility in complicated environment. Therefore, efforts have been devoted to the development of optical fiber force sensors. The developing categories include fiber gratings [7], [8], Fabry-perot interferometers (FPI) [9], [10], [11], Mach-Zehnder interferometers (MZI) [12] and optical fibers [13], [14]. In 2018, by using single-mode tilted fiber gratings, Shen et al. experimentally demonstrated the tension measuring of liquids and achieved milli-Newton-level force measurement [15]. In 2019, Jitendra Narayan Dash et al. fabricated a force sensor based on a micro-length single-mode fiber incorporated in a cleave micro-air cavity and the maximum force sensitivity is experimentally demonstrated to be 14.2 pm/mN and the measurement range of the sensor covers from 0 to 10 N [16]. In 2020, Simon Pevec and Denis Donlagic, reported a thin silica diaphragm created at the optical fiber tip to form a sealed Fabry-Perot interferometer and achieved a measurement range of ~0.6 mN and a force resolution of ~0.6 μN [11]. Despite of such remarkable force resolution, the fabrication is complicated and the measurement range is small.

Whispering gallery mode (WGM) resonator has attracted wide attention for its remarkable performance which stems from high quality factor, small mode volumn and high optical energy density. Applied as a precise measurement platform, various applications have been performed including biomedical sensing [17], [18], microfluid measurement [19], [20] and temperature sensing [21]. In recently years, owning to the development and convergence of optimized photonics, optomechanics and MEMS/NEMS technologies [22], a new category of integrated silicon cantilever probe using a microdisk resonator is experimentally demonstrated and can be used for atomic force microscopy (AFM) [23], [24], [25]. However, this type of microdisk resonators usually possesses low quality factor Q, and by reason of the instability of coupling, the Q factor is highly susceptible to interference during detection.

In this work, we propose a novel miniature force sensor based on a WGM resonator. The resonator consists of a microbubble support by a silica capillary and a probe on the tip of the bubble. The overall size of the sensor is less than 300 μm × 125 μm. Predominantly, the sensor exhibits a Q factor of 1.10×10^7 with a force sensitivity of 19.7 pm/mN. The dynamic range was

Manuscript received 6 August 2023; revised 28 September 2023 and 10 October 2023; accepted 14 October 2023. Date of publication 18 October 2023; date of current version 4 March 2024. This work was supported in part by the National Natural Science Foundation of China (NSFC) under Grants 62175165 and U1913212, in part by Guangdong Basic and Applied Basic Research Foundation under Grant 2021A1515011834, in part by Shenzhen Science and Technology Program under Grant JCYJ20210324120403009, and in part by the Shenzhen Science and Technology Program, Shenzhen Key Laboratory of Ultrafast Laser Micro/Nano Manufacturing under Grant ZDSYS20220606100405013. *(Bonan Liu and Qiang Zhang contributed equally to this work.) (Corresponding author: Shen Liu.)*

Bonan Liu, Shen Liu, Changrui Liao, Jun He, and Yiping Wang are with the Shenzhen Key Laboratory of Photonic Devices and Sensing Systems for Internet of Things, College of Physics and Optoelectronic Engineering, Shenzhen University, Shenzhen 518060, China, and also with the Guangdong and Hong Kong Joint Research Centre for Optical Fibre Sensors, Shenzhen University, Shenzhen 518060, China (e-mail: ssamliu@163.com; shenliu@szu.edu.cn; cliao@szu.edu.cn; hejun07@szu.edu.cn; ypwang@szu.edu.cn).

Qiang Zhang and Junlan Zhong are with the Shenzhen Key Laboratory of Photonic Devices and Sensing Systems for Internet of Things, College of Physics and Optoelectronic Engineering, Shenzhen University, Shenzhen 518060, China (e-mail: 1900453038@email.szu.edu.cn; zhongjunlan@email.szu.edu.cn).

Color versions of one or more figures in this article are available at https://doi.org/10.1109/JLT.2023.3325726.

Digital Object Identifier 10.1109/JLT.2023.3325726

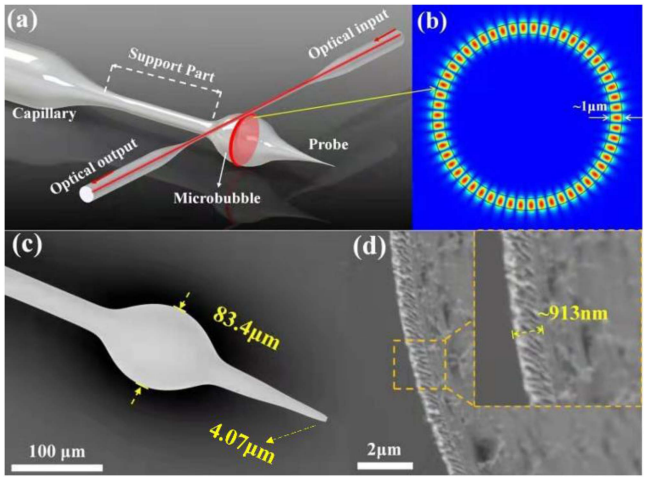

Fig. 1. (a) Schematic of the MPR. (b) Typical calculated distribution of the optical modes at the cross section of the microbubble with a wall thickness of 1 μm. (c) The SEM image of the MPR. The diameter of the equatorial plane is ~83.4 μm. (d) The cut-plane SEM image of the microbubble showing a wall thickness of ~913 nm.

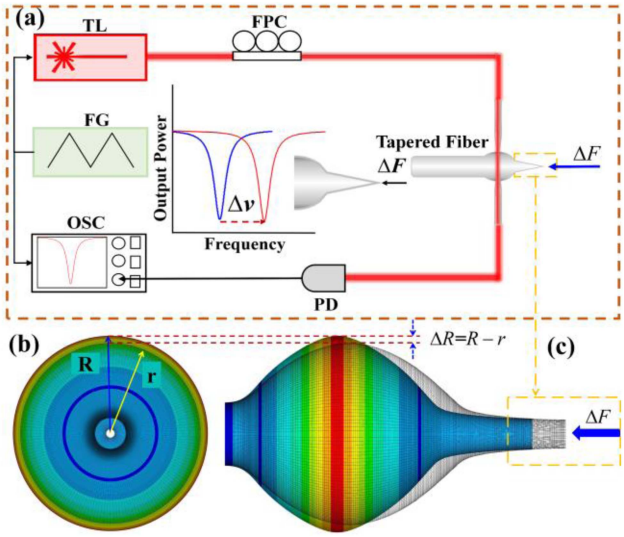

Fig. 2. (a) Schematic of the experimental setup. FPC: Fiber polarization controller. The inset shows a schematic diagram of applied force, the blue arrow indicates the forced direction. (b) The corresponding deformation of the MPR under the force for the transverse section. (c) The side view of stress distribution contours.

evaluated to be 0-36 mN. The detect limit (DL) is calculated to be 1.3 μN. The proposed sensor exhibits considerable performance but requires only simple fabrication. High force resolution and spatial resolution are achieved simultaneously, which offers intriguing ideas on micro force measurement.

II. Fabrication and Characterization

A schematic is provided to illustrate the structure of the MPR, as shown in Fig. 1(a). The microbubble plays a role of resonator with a tapered fiber placed on the equatorial plane. Transmitting in the tapered fiber, the light is able to couple into the bubble and generate WGM resonance therein. The optical field on the equatorial plane was simulated and found to be distributed across the inner and outter area of the bubble, which is shown in Fig. 1(b). The MPR illustrated here has a diameter of 83.4 μm, and its wall thickness was examined to be 913 nm after cutting open by femtosecond laser. The probe locates on the tip of the microbubble and has a diameter of 4.07 μm. This offers a micron-level spatial resolution. The geometry features of the microbubble including wall thickness and diameter are crucial factors for the resonator performance [26].

The MPR was fabricated using the same method as [27]. The capillary selected has an outer diameter of 350 μm and an inner diameter of 250 μm using CO_2 laser machining platform. A capillary was firstly mounted on two translation stages and heated in the middle by two cross-propagated laser beams. A tapered structure with a waist diameter of 25 μm was formed by pulling the capillary on both sides. Being pressurized and heated, the waist became soften and expanded to a bubble. After relocating the laser spots on one of the support parts, the stage pulled again until the support part broke. The MPR was thereby obtained, where the wall thickness of the formed bubble depends highly on the internal pressure and laser power while the power and the pulling speed determines the length of the probe. The spectra were measured using the experimental setup showed in Fig. 2(a). A function generator (FG) with a scanning range up to 30 GHz was connected to a tunable laser (TL, New Focus TLB-6712). The output was collected by a 400 MHz photon detector (PD) which was connected to a digital oscilloscope (OSC). To avoid contamination and perturbation from ambient environment, the setup was placed in a clean chamber during measurement.

As force is applied towards the sensor, the probe introduces the force to the microbubble, which leads to a deformation in the equatorial plane diameter, as shown in Fig. 2(b). During this process, the equator exhibits the major deformation while the probe and the support part shows a tiny deformation. The radius variation $\Delta R = R\text{-}r$ literally refers to the difference between the diameters of before and after the force applying. Such diameter deformation of the microbubble can be read out as dip shifts on the oscilloscope. The wavelength shift can be expressed as [28]:

$$\Delta\lambda \approx \Delta R\lambda / R_0 \tag{1}$$

where R_0 refers to the initial equatorial plane diameter of the microbubble. Therefore, noticeable frequency shift can be observed under various force applied. For the selected MPR shown in Fig. 3(a), a high Q factor of 1.10×10^7 is obtained under critical coupling.

The relationship between the applied force and the deformation of the MPR was quantified using the Nano-Indenter (Hysitron, TI-950) (see Fig. 4). The MPR was firstly mounted on tailored holder with the probe pointed upwards. The holder was fixed on the object stage. The standard probe of the indenter was connected to a transducer and was placed on the top with its tip pointed downwards. During the indentation process, the standard probe continually pressed the MPR and the correlation between the deformation and the force applied can be obtained.

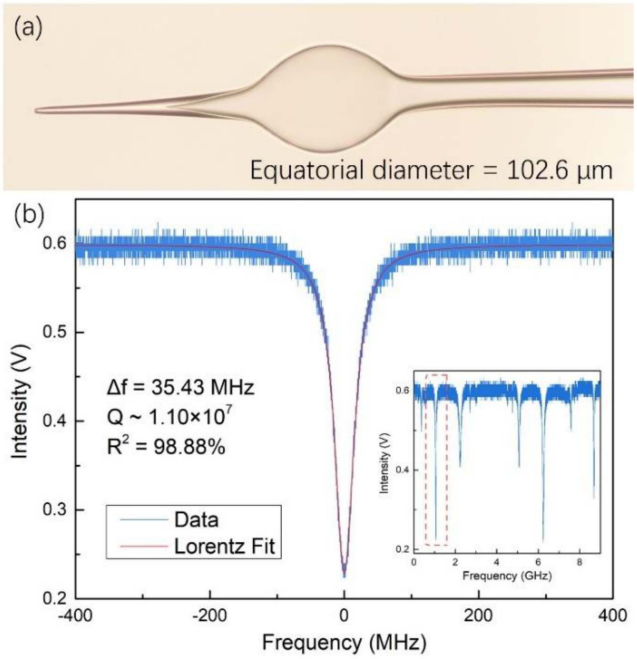

Fig. 3. (a) The microscope image of an MPR. (b) A typical resonance dip of the MPR at 772.495 nm. The red line is Lorenz fitting with linewidth of 35.43 MHz corresponding to a Q factor of 1.10×10^7.

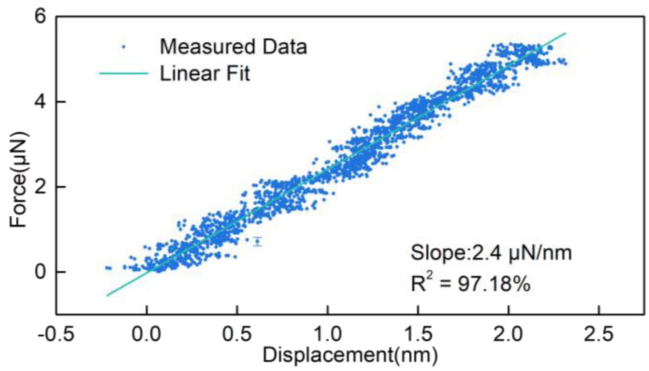

Fig. 4. Stiffness coefficient of the MPR. Error bar has been added to one point to demonstrate an error level of ± 0.1 μN.

From the curve, the stiffness coefficient of the sample can be found to be 2.4 μN/nm.

III. Results and Discussion

A force was applied on the MPR and increased from 0 to 1680 μN corresponding to an induced displacement from 0 to 700 nm. A metal board fixed on the translation stage was used to press the microbubble probe. The tapered fiber was in contact with the microbubble in order to ensure a stable coupling as the forced applied. The sensitivity is found to be 19.7 pm/mN with a linearity of 99.68%. Fig. 5(b) shows that the resonance dip can shift over a free spectral range (FSR) yielding a dynamic range of 0-36 mN. By reducing the wall thickness of the bubble and

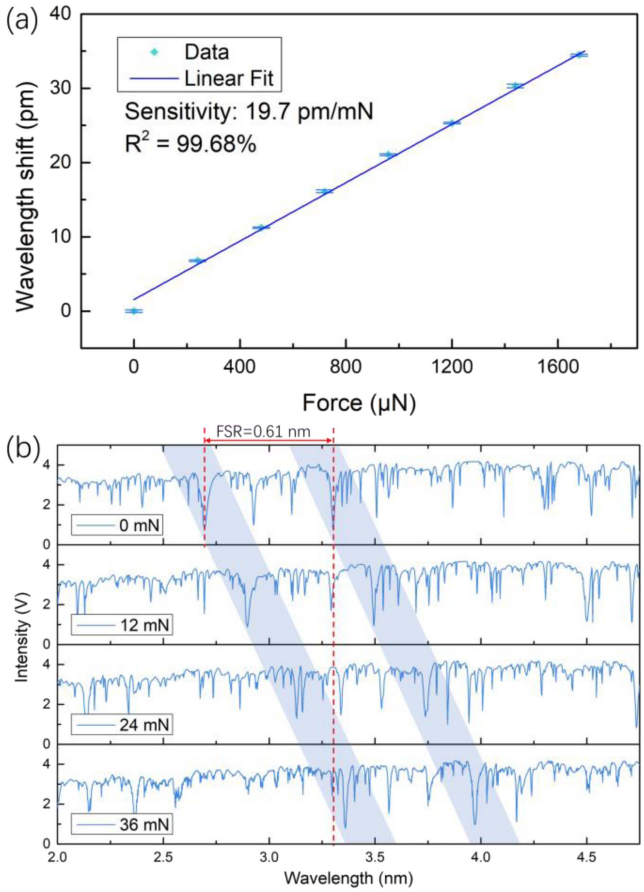

Fig. 5. (a) Dip shift versus force applied with linear fit. The error bar is obtained by repeating the same test for 3 times. (b) Evolution of transmission spectra of the MPR as the force increased from 0 to 36 mN.

optimizing the shape of the bubble, the sensitivity can be further improved [26], [29].

The DL of the sensor is known as the smallest applied-force variation that can be accurately measured. The DL can be expressed as [30]

$$DL = \frac{R}{S} \tag{2}$$

where S and R represent the sensitivity and resolution of the sensor, respectively. The latter can be approximately solved by individual noise variances ($R = 3\sigma$), i.e., [30]

$$\sigma \approx \frac{\Delta\lambda_F}{4.5\,(SNR^{0.25})} \tag{3}$$

$\Delta\lambda_F$ refers to the FWHM of the fringe. Knowing the FWHM of the fringe is 0.07 pm (from Fig. 3(b)), the DL can be calculated to be 1.3 μN where a measured SNR value of 10.8 dB was used. It can be known from (3) that the DL is strongly related to the SNR. If a typical SNR value of 60 dB is selected [30], to evaluate the exact performance of the device, the DL can reach 74.9 nN. This makes the proposed sensor a promising candidate in detecting tiny forces.

To verify the measurement accuracy of the sensor, a measurement of the Young's modulus on a SMF was conducted. In

TABLE I
PERFORMANCE COMPARISON OF REPORTED FORCE SENSOR

Type	Sensitivity	Dynamic range	Size of the device
PCF Sagnac interferometer [33]	0.016×10^{-3} pm/μN	0-392 mN	125 μm × 3 cm
FPI probe [11]	360 pm/μN	0-0.6 mN	800 μm × 105 μm
FPI [16]	0.0142 pm/μN	0-10000 mN	400 μm × 205 μm
FBG with diaphragm [34]	442×10^{-3} pm/μN	0-4900 mN	-
Microfiber asymmetrical FPI [35]	0.221 pm/μN	-	20 mm × 7.3 μm
FP cuboid cavity [36]	0.026 pm/μN	0-500 mN	18 μm × 60 μm
FP micro-cavity plugged by cantilever taper [37]	0.842 pm/μN	0-400 mN	1360 μm × 125 μm
Balloon-like interferometer [38]	24.9 pm/μN	0-1.464 mN	24 mm × 14 mm
Fiber-tip polymer clamped-beam probe [9]	1510 pm/μN	0-2.9 mN	68 μm × 100 μm
This work	0.0197 pm/μN	0-36 mN	300 μm × 125 μm

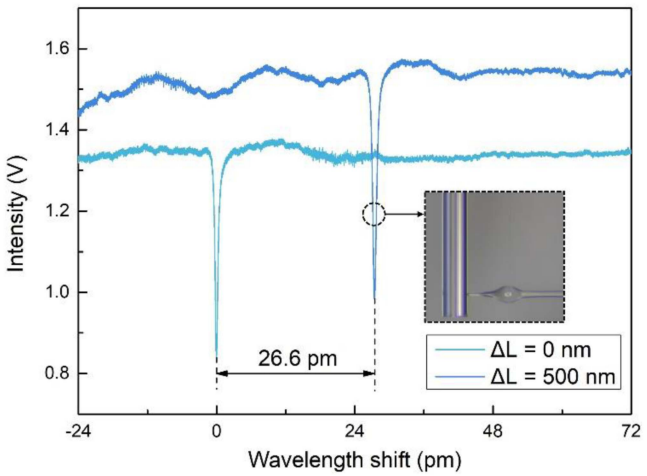

Fig. 6. Wavelength shift of the dip of interest as SMF deflects from 0 to 500 nm. The inset shows a CCD image of pushing the SMF.

operation, one end of the SMF was fixed by the sample holder and the other end was deflected by the sensor (see Fig. 6 inset). In this case, the SMF can be regarded as a cantilever beam with one end fixed. The diameter of the probe was much smaller than that of SMF yielding that such process can be regarded as a point load induced deformation which fits the following relation [31]:

$$\Delta L = \frac{FL^3}{3EI} \tag{4}$$

ΔL refers to the deflection of the SMF. L is the length of the SMF. The point load on the end of the SMF is denoted as F. E and I refer to the Young's modulus of the SMF and the second moment of area of the SMF, respectively. Standard parameters of SMF were used in the calculations, including a diameter of 125 μm, a length of 1 mm and an SMF deflection ΔL (obtained from the motor controller). The circular second moment of area follows [32]:

$$I = \frac{\pi d^4}{64} \tag{5}$$

where d, in units of mm, is the diameter of the SMF. Knowing a 500 nm deformation causes a wavelength shift of 26.6 pm, the force received by SMF can be obtained using the result in Fig. 6. The Young's modulus of the SMF was calculated to be 75.1 GPa which is just slightly different from 73 GPa, the actual Young's modulus of SMF. The measurement error is 2.89% falling into the allowable range of error.

Table I shows a comparison of the resonator proposed and other types of force sensor. Despite the device in this work is not superior in all aspects, it offers a novel solution for force measurement. With hollow structure, a high spatial resolution probe, and the using of WGM MPR as a platform, the device has the potential to be applied in various fields.

IV. CONCLUSION

To conclude, a novel miniature force sensor based on a MPR was proposed. The sensor is compact in size, and achieves a force sensitivity of 19.7 pm/mN. The highest quality factor obtained is 1.10×10^7. The dynamic range of the sensor was evaluated to be 0-36 mN while the DL is calculated to be 1.3 μN. In addition, high force resolution and spatial resolution are achieved simultaneously. With considerable performance and reliable measurement on Young's modulus, the sensor proposed exhibits a potential in micro-force sensing, material examination, surface imaging and other related domains.

REFERENCES

[1] H. Conrad et al., "A small-gap electrostatic micro-actuator for large deflections," *Nature Commun.*, vol. 6, no. 1, Dec. 2015, Art. no. 10078.
[2] H. Guo et al., "Artificially innervated self-healing foams as synthetic piezo-impedance sensor skins," *Nature Commun.*, vol. 11, no. 1, Nov. 2020, Art. no. 5747.
[3] K. Uhrig et al., "Optical force sensor array in a microfluidic device based on holographic optical tweezers," *Lab Chip*, vol. 9, no. 5, pp. 661–668, Mar. 2009.
[4] M. Siskins et al., "Sensitive capacitive pressure sensors based on graphene membrane arrays," *Microsystems Nanoeng.*, vol. 6, no. 1, 2020, Art. no. 102.
[5] T. Sun et al., "Decoding of facial strains via conformable piezoelectric interfaces," *Nature Biomed. Eng.*, vol. 4, no. 10, pp. 954–972, Oct. 2020.
[6] X. Han et al., "Novel resonant pressure sensor based on piezoresistive detection and symmetrical in-plane mode vibration," *Microsyst. Nanoeng.*, vol. 6, no. 1, p. 95, 2020.
[7] K. M. Chung, Z. Liu, C. Lu, and H.-Y. Tam, "Highly sensitive compact force sensor based on microfiber Bragg grating," *IEEE Photon. Technol. Lett.*, vol. 24, no. 8, pp. 700–702, Apr. 2012.

[8] B. Xu et al., "Simultaneous measurement of torsion and strain at high temperature by using a highly birefringent cladding fiber Bragg grating," *Opt. Exp.*, vol. 30, no. 16, pp. 28710–28719, Aug. 2022.
[9] M. Zou et al., "Fiber-tip polymer clamped-beam probe for high-sensitivity nanoforce measurements," *Light Sci. Appl.*, vol. 10, no. 1, p. 171, Aug. 2021.
[10] A. J. Thompson, M. Power, and G. Z. Yang, "Micro-scale fiber-optic force sensor fabricated using direct laser writing and calibrated using machine learning," *Opt. Exp.*, vol. 26, no. 11, pp. 14186–14200, May 2018.
[11] S. Pevec and D. Donlagic, "Miniature all-fiber force sensor," *Opt. Lett.*, vol. 45, no. 18, pp. 5093–5096, Sep. 2020.
[12] L. Zhao, Y. Zhang, Y. Chen, Y. Chen, G. Yi, and J. Wang, "A fiber strain sensor with high resolution and large measurement scale," *IEEE Sensors J.*, vol. 20, no. 6, pp. 2991–2996, Mar. 2020.
[13] H. Zang, X. Zhang, H. Zhang, B. Zhu, and S. Fatikow, "A novel force sensor based on optical fibers used for semicircular flexure beam unit," *IEEE Trans. Instrum. Meas.*, vol. 71, 2022, Art. no. 9502010.
[14] F. Arcadio, L. Zeni, and N. Cennamo, "Exploiting plasmonic phenomena in polymer optical fibers to realize a force sensor," *Sensors*, vol. 22, no. 6, Mar. 2022, Art. no. 2391.
[15] C. Shen et al., "Measurements of milli-Newton surface tension forces with tilted fiber Bragg gratings," *Opt. Lett.*, vol. 43, no. 2, pp. 255–258, Jan. 2018.
[16] J. N. Dash, Z. Liu, D. S. Gunawardena, and H. Y. Tam, "Fabry–Perot cavity-based contact force sensor with high precision and a broad operational range," *Opt. Lett.*, vol. 44, no. 14, pp. 3546–3549, Jul. 2019.
[17] Y. N. Zhang, T. Zhou, B. Han, A. Zhang, and Y. Zhao, "Optical bio-chemical sensors based on whispering gallery mode resonators," *Nanoscale*, vol. 10, no. 29, pp. 13832–13856, Aug. 2018.
[18] X. Zhao et al., "Optical whispering-gallery-mode microbubble sensors," *Micromachines*, vol. 13, no. 4, p. 592, Apr. 2022.
[19] K. H. Kim et al., "Cavity optomechanics on a microfluidic resonator with water and viscous liquids," *Light: Sci. Appl.*, vol. 2, no. 11, 2013, Art. no. e110.
[20] B. Yao et al., "Graphene-enhanced Brillouin optomechanical microresonator for ultrasensitive gas detection," *Nano Lett.*, vol. 17, no. 8, pp. 4996–5002, Aug. 2017.
[21] J. Liao and L. Yang, "Optical whispering-gallery mode barcodes for high-precision and wide-range temperature measurements," *Light Sci. Appl.*, vol. 10, no. 1, Feb. 2021, Art. no. 32.
[22] L. Wei et al., "The recent progress of MEMS/NEMS resonators," *Micromachines*, vol. 12, no. 6, Jun. 2021, Art. no. 724.
[23] J. Chae et al., "Nanophotonic atomic force microscope transducers enable chemical composition and thermal conductivity measurements at the nanoscale," *Nano Lett.*, vol. 17, no. 9, pp. 5587–5594, Sep. 2017.
[24] P. E. Allain et al., "Optomechanical resonating probe for very high frequency sensing of atomic forces," *Nanoscale*, vol. 12, no. 5, pp. 2939–2945, Feb. 2020.
[25] K. Srinivasan, H. Miao, M. T. Rakher, M. Davanco, and V. Aksyuk, "Optomechanical transduction of an integrated silicon cantilever probe using a microdisk resonator," *Nano Lett.*, vol. 11, no. 2, pp. 791–797, Feb. 2011.
[26] B. Xu, M. Chen, K. Yang, Y. Guo, D. N. Wang, and C. L. Zhao, "Ultra-high sensitivity strain sensor based on biconical fiber with a bulge air-bubble," *Opt. Lett.*, vol. 46, no. 8, pp. 1983–1986, Apr. 2021.
[27] B. Liu et al., "Microbubble-probe WGM resonators enable displacement measurements with high spatial resolution," *Opt. Lett.*, vol. 48, no. 7, pp. 1922–1925, 2023.
[28] M. Sumetsky, Y. Dulashko, and R. S. Windeler, "Super free spectral range tunable optical microbubble resonator," *Opt. Lett.*, vol. 35, no. 11, pp. 1866–1868, Jun. 2010.
[29] S. Liu et al., "Strain-based tunable optical microresonator with an in-fiber rectangular air bubble," *Opt. Lett.*, vol. 43, no. 17, pp. 4077–4080, Sep. 2018.
[30] I. M. White and X. Fan, "On the performance quantification of resonant refractive index sensors," *Opt. Exp.*, vol. 16, no. 2, pp. 1020–1028, Jan. 2008.
[31] W. Ding, Z. Guo, and R. S. Ruoff, "Effect of cantilever nonlinearity in nanoscale tensile testing," *J. Appl. Phys.*, vol. 101, no. 3, Feb. 2007, Art. no. 034316.
[32] K. V. Namjoshi and P. P. Biringer, "Low-frequency Eddy-current loss estimation in long conductors by using the moment of inertia of cross sections," *IEEE Trans. Magn.*, vol. 24, no. 5, pp. 2181–2185, Sep. 1988.
[33] Q. Liu, L. Xing, Z. Wu, L. Cai, Z. Zhang, and J. Zhao, "High-sensitivity photonic crystal fiber force sensor based on Sagnac interferometer for weighing," *Opt. Laser Technol.*, vol. 123, 2020, Art. no. 105939.
[34] R. Li et al., "A diaphragm-type highly sensitive fiber Bragg grating force transducer with temperature compensation," *IEEE Sensors J.*, vol. 18, no. 3, pp. 1073–1080, Feb. 2018.
[35] Y. Gong et al., "Highly sensitive force sensor based on optical microfiber asymmetrical Fabry-Perot interferometer," *Opt. Exp.*, vol. 22, no. 3, pp. 3578–3584, 2014.
[36] Y. Liu, S. Qu, W. Qu, and R. Que, "A Fabry–Perot cuboid cavity across the fibre for high-sensitivity strain force sensing," *J. Opt.*, vol. 16, no. 10, 2014, Art. no. 105401.
[37] Y. Liu, C. Lang, X. Wei, and S. Qu, "Strain force sensor with ultra-high sensitivity based on fiber inline Fabry-Perot micro-cavity plugged by cantilever taper," *Opt. Exp.*, vol. 25, no. 7, pp. 7797–7806, 2017.
[38] Y. Wu et al., "Highly sensitive force sensor based on balloon-like interferometer," *Opt. Laser Technol.*, vol. 103, pp. 17–21, 2018.

Bonan Liu received the B.E. degree in optoelectronic information engineering from Shenzhen University, Shenzhen, China, in 2016, and the M.E. degree in telecommunication engineering from the University of New South Wales, Sydney NSW, Australia, in 2019. He is currenlty working toward the Ph.D. degree majoring in optics engineering with the College of Physics and Optoelectronic Engineering, Shenzhen University. His research interests include fiber-based micro cavity and tilted fiber gratings.

Qiang Zhang was born in Hebei, China, in 1997. He received the B.S. degree in opto-electronics information science and engineering from Xiangtan University, Xiangtan, China, in 2019, and the M.E. degree in optics engineering from Shenzhen University, Shenzhen, China, in 2022. He is currently working toward the Doctoral degree from the University of Macau, Macau, China, with a research focus on intelligent optical measurement. He is also pursuing a joint Doctoral Program with Shenzhen University, Shenzhen, China, and the University of Macau.

Shen Liu was born in Henan, China, in 1986. He received the B.Eng. degree in electronic and information engineering from PLA Air Force No.1 Aviation University, Changchun, China, in 2008, the M.S. degree in circuit and system from the Chongqing University of Posts and Telecommunications, Chongqing, China, in 2013, and the Ph.D. degree in optics from Shenzhen University, Shenzhen, China, in 2017. From 2017 to 2018, he was with Aston University, Birmingham, U.K., as a Postdoctoral Fellow. Since 2018, he has been with Shenzhen University, Shenzhen, as an Associate Professor. His current research interests include optical fiber sensors, WGMs resonator, and cavity optomechanics.

Changrui Liao (Member, IEEE) received the B.S. degree in optical information science and technology and the M.E. degree in physical electronics from the Huazhong University of Science and Technology, Wuhan, China, in 2005 and 2007, respectively, and the Ph.D. degree in optical engineering from the Hong Kong Polytechnic University, Hong Kong, in 2012. He is currently a Distinguished Professor with the College of Physics and Optoelectronic Engineering, Shenzhen University, Shenzhen, China, and holds the position of the Deputy Director of Guangdong and Hong Kong Joint Research Center for Optical Fiber Sensors. Since 2012, he has been with Shenzhen University. His research interests include optical fiber sensor, femtosecond laser micromachining, and MOEMS.

Junlan Zhong was born in Jiangxi, China, in 1990. She received the B.E. degree of Engineering in biomedical engineering from Jinggangshan University, Ji'an, China, in 2013, the M.S. degree of Engineering in biomedical engineering from Shenzhen University, Shenzhen, China, in 2016, and the Ph.D. degree of Philosophy in environment studies from the University of Tsukuba, Tsukuba, Japan, in 2017. Since 2020, she has been with Shenzhen University, as a Research Fellow. Her research interests include terahertz spectroscopy, WGMs resonators, and biosensors.

Jun He was born in Hubei, China, in 1985. He received the B.Eng. degree in electronic science and technology from Wuhan University, Wuhan, China, in 2006, and the Ph.D. degree in electrical engineering from the Institute of Semiconductors, Chinese Academy of Sciences, Beijing, China, in 2011. From 2011 to 2013, he was with Huawei Technologies, Shenzhen, China, as a Research Engineer. From 2013 to 2015, he was affiliated with Shenzhen University, Shenzhen, as a Postdoctoral Research Fellow. From 2015 to 2016, he was with The University of New South Wales, Sydney, NSW, Australia, as a Visiting Fellow. Since 2017, he has been with Shenzhen University, Shenzhen, as an Distinguished Professor. His research interests include optical fiber sensors, fiber Bragg gratings (FBGs), and fiber lasers. He is a member of the Optical Society of America.

Yiping Wang (Senior Member, IEEE) was born in Chongqing, China, in 1971. He received the B.Eng. degree in precision instrument engineering from the Xi'an Institute of Technology, Xi'an, China, in 1995, and the M.S. and Ph.D. degrees in optical engineering from Chongqing University, Chongqing, China, in 2000 and 2003, respectively. From 2003 to 2005, he was with Shanghai Jiao Tong University, Shanghai, China, as a Postdoctoral Fellow. From 2005 to 2007, he was with the Hong Kong Polytechnic University, Hong Kong, as a Postdoctoral Fellow. From 2007 to 2009, he was with the Institute of Photonic Technology, Jena, Germany, as a Humboldt Research Fellow. From 2009 to 2011, he was with the Optoelectronics Research Centre (ORC), University of Southampton, Southampton, U.K., as a Marie Curie Fellow. Since 2012, he has been with Shenzhen University, Shenzhen, China, as a Distinguished Professor. His research interests include optical fiber sensors, fiber gratings, and photonic crystal fibers. Dr. Wang is a Senior Member of Optical Society of America, and Chinese Optical Society.